BMC Cancer

RESEARCH

Open Access

Exploring MPC1 as a potential ferroptosis-linked biomarker in the cervical cancer tumor microenvironment: a comprehensive analysis

Miao Li[1†], Tianhan Xu[1†], Rui Yang[2], Xiaoyun Wang[1*], Jiawen Zhang[1,3*] and Sufang Wu[1*]

Abstract

Background The increasing problems of drug and radiotherapy resistance in cervical cancer underscores the need for novel methods for its management. Reports indicate that the expression of MPC1 may be associated with the tumor microenvironment and the occurrence of ferroptosis in cervical cancer. The objective of this study was to visually illustrate the prognostic significance and immunological characterization of MPC1 in cervical cancer.

Methods The expression profile and prognostic significance of MPC1 were analyzed using various databases, including UALCAN, TIMER2, GEPIA2, and Kaplan–Meier Plotter. TISIDB, TIMER2, and immunohistochemical analysis were used to investigate the correlation between MPC1 expression and immune infiltration. GO enrichment analysis, KEGG analysis, Reactome analysis, ConsensusPathDB, and GeneMANIA were used to visualize the functional enrichment of MPC1 and signaling pathways related to MPC1. The correlation analysis was carried out to examine the relationship between MPC1 and Ferroptosis gene in TIMER 2.0, ncFO, GEPIA Database and Kaplan–Meier Plotter.

Results We demonstrated that the expression levels of MPC1 in cervical cancer tissues were lower than those in normal cervical tissues. Kaplan–Meier survival curves showed shorter overall survival in cervical cancer patients with low levels of MPC1 expression. The expression of MPC1 was related to the infiltrating levels of tumor-infiltrating immune cells in cervical cancer. Moreover, MPC1 expression was associated with the iron-mediated cell death pathway, and several important ferroptosis genes were upregulated in cervical cancer cells. Furthermore, after knocking down MPC1 in HeLa cells, the expression of these genes decreased.

Conclusion These findings indicate that MPC1 functions as a prognostic indicator and plays a role in the regulation of the ferroptosis pathway in cervical cancer.

Keywords Cervical cancer, MPC1, Ferroptosis, Prognosis, Immune response

†Miao Li and Tianhan Xu contributed equally to this work.

*Correspondence:
Xiaoyun Wang
littleyun2007@sina.com
Jiawen Zhang
jwzhang929@163.com
Sufang Wu
wsf_sfph@sjtu.edu.cn

[1]Department of Obstetrics and Gynecology, Shanghai General Hospital, Shanghai Jiao Tong University School of Medicine, Shanghai, People's Republic of China
[2]Department of Obstetrics and Gynaecology, the First Affiliated Hospital of Guangzhou Medical University, Guangzhou, Guangdong 510120, China
[3]Reproductive Medicine Center, Department of Obstetrics and Gynecology, Shanghai General Hospital, Shanghai Jiao Tong University School of Medicine, Shanghai, People's Republic of China

Introduction

In spite of the implementation of pre-cancerous screening and the endorsement of human papillomavirus vaccines, cervical cancer remains the primary contributor to cancer-related mortality among women residing in developing regions [1, 2]. According to the latest Global Cancer Statistic 2020 (GLOBOCAN), cervical cancer continues to be the fourth most common cancer worldwide, with 604,127 estimated new cases and at least 341,831 deaths due to this disease [3, 4]. The therapeutic modalities accessible for cervical cancer encompass surgical interventions, radiation therapy, chemotherapy, or a combination of these modalities. Nevertheless, late or recurrent cervical cancer exhibits a comparatively limited response to these therapeutic approaches and presents a less favorable prognosis [5]. Consequently, novel therapies are needed for the treatment of cervical cancer.

Ferroptosis, an iron-dependent and regulated mode of cell death, has incited significant attention among cancer research circles. This interest has been fueled by a growing body of evidence suggesting that ferroptosis may be a promising avenue for the development of novel cancer therapies and treatments [6]. This modality of cell death is different from other forms of cell death. It is a death process driven by iron-dependent phospholipid peroxidation [7, 8]. Ferroptosis is involved in the activities of several tumor suppressors, such as p53 and BRCA1-associated protein 1 (BAP1). Therefore, it has been established as a natural barrier to cancer development [6].

The molecular genetic identification of the mitochondrial pyruvate carrier (MPC) is represented in the form of a gene card (https://www.genecards.Org/), outlining a heterodimeric complex composed of protein subunits MPC1 and MPC2 [9]. MPC has also emerged as a target for therapeutic intervention in a variety of diseases characterized by altered mitochondrial and intermediary metabolism [10]. MPC1 is a tumor suppressor in diseases, such as colorectal carcinoma (CRC) [11], hepatocellular carcinoma (HCC) [12, 13], glioblastoma (GBM) [14], prostate adenocarcinoma [10], among others. An increase in the expression of MPC is closely linked to a favorable prognostic outcome, whereas in the context of BRCA, diminished MPC1 expression is substantially correlated with a decrease in overall survival duration [15]. However, the specific mechanism underlying the role of MPC1 in cervical cancer remains unclear.It is anticipated that the expression of MPC1 is diminished in cervical cancer. Individuals with elevated levels of MPC1 may experience a more favorable prognosis. This necessitates further investigation. Using the Public Bioinformation Database, we aimed to determine the functional roles of MPC1 in the progression and prognosis of patients with cervical cancer. Additionally, we conducted a systematic analysis of the biological functions of MPC1. We also evaluated whether aberrantly expressed MPC1 might affect the immune response and ferroptosis in patients with cervical cancer. Overall, our research presents an opportunity to enhance current understanding of the potential biological significance of MPC1 in cervical cancer.

Materials and methods

Identification of differentially expressed genes

The normalized gene expression data for cervical cancer (GSE7803, GSE9750, and GSE39001) were downloaded from the Gene Expression Omnibus [16](GEO, https://www.ncbi.nlm.nih.gov/geo/). The differentially expressed genes (DEGs) of each dataset were identified using the R package 'limma' according to the following criteria: p-value < 0.05 and $|\log FC| \geq 1$. Overall, 484 ferroptosis-related genes were obtained from FerrDb [17].

Weighted correlation network analysis (WGCNA) of TIP cervical cancer data

The R package 'WGCNA' was used to construct a weighted co-expression network. Normalized TCGA-CESC data was used as a data matrix for WGCNA. The cancer-immunity cycle scores of cervical cancer samples were obtained from the Tracking Tumor Immunophenotype (TIP) database [18] (http://biocc.hrbmu.edu.cn/TIP/index.jsp) as immune processes module phenotypes for WGCNA. A fit β value of 10 was selected to generate a scale-free co-expression network. Based on the topological overlap, the average-linkage hierarchical clustering method was used to cluster genes. According to the standard of the hybrid dynamic shearing tree, the minimum number of genes in each gene network module was set to 100. The eigengenes of each module were calculated, and the height was set to 0.25. Overall, 13 modules were clustered; further, the gray module comprises genes that could not be clustered into other modules. According to the eigengenes of each module, the correlation between these modules and each immune processes phenotype was calculated and displayed using a heatmap. The purple and turquoise modules were selected for subsequent analysis because they were significantly associated with immune cell recruitment, which containing 2248 genes.

Online database analysis

The UALCAN Database (http://ualcan.path.uab.edu/) and GEPIA Database (http://gepia.cancer-pku.cn/index.html) were used to assess the expression of MPC1 in patients with cervical cancer. To evaluate the prognostic value of MPC1 mRNA expression in cervical cancer, MPC1 was entered into the TISIDB (http://cis.hku.hk/TISIDB/) [19], OncoLnc (http://www.oncolnc.org/) [20], and Kaplan–Meier Plotter (http://kmplot.com/analysis/index) [21] to obtain survival plots. Hazard ratios (HR)

with 95% confidence intervals and log-rank P values were calculated on the web page. The correlations between MPC1 expression and infiltrated immune cells and markers in cervical cancer tissues were analyzed using TIMER2.0 (http://timer.cistrome.org/). Pearson correlation was used to analyze the correlation between MPC1 expression and immune cells and was conducted using R software (4.2.1). The Sangebox database(http://past20.sangerbox.com/Gene) was utilized to analyze the correlation between MPC1 and immune checkpoints. The single-cell sequencing (scRNA-seq) datasets of CESC were acquired from the Tumor Immune Single-cell Hub (TISCH2, http://tisch.comp-genomics.org/) according to the website's guidelines.

Clinical specimens and and ethical approval

The group comprised 32 paired samples of cervical cancer and matched normal cervix tissues. Within the cervical cancer specimens, 23 cases were devoid of lymphatic metastasis while 7 cases exhibited lymphatic metastasis. The specimens were sourced from the Department of Obstetrics and Gynecology at Shanghai General Hospital and promptly preserved in formalin. All clinicopathological diagnoses were validated by two pathologists in accordance with the World Health Organization (WHO) classification guidelines. The current investigation received approval from the Ethics Committee of Shanghai General Hospital. Prior to their participation in the study, all subjects provided written informed consent.

Immunohistochemical analysis

The tissue microarray (TMA) was boiled in 10 mM sodium-citrate buffer for 5 min to retrieve antigens after dewaxing and rinsing. The TMA was then blocked in 4% hydrogen peroxide for 10 min to prevent interference from endogenous peroxidase activity. Afterwards, the TMA was incubated with the anti-MPC1 rabbit polyclonal antibody (1:250, Affinity, Jiangsu, China) at 4 °C overnight. The next day, the TMA was incubated with secondary antibodies at room temperature for 30 min and stained with DAB and hematoxylin. Lastly, the TMA was covered with coverslips for microscopic examination. Staining intensity was scored on the following scale: 0 (negative staining), 1 (weak staining), 2 (moderate staining), and 3 (strong staining). The proportion of positively stained areas was evaluated using five levels: 0 (<5%), 1 (5–25%), 2 (25–50%), 3 (50–75%), and 4 (>75%). The final score was the product of the above two indicators.

Cell lines and cell culture

Human cervical cancer cell lines HeLa, SiHa, C33A, CaSki, and Me180, along with the normal cervical epithelial cell line H8, were procured from the Type Culture Collection of the Chinese Academy of Sciences (Shanghai, China). The cells were cultured in Dulbecco's modified Eagle's medium (DMEM medium; GIBCO from Thermo Fisher, USA) supplemented with 10% fetal bovine serum (FBS, GIBCO) and 1% penicillin–streptomycin, and maintained in a humidified atmosphere of 5% CO2 at 37 °C.

RNA extraction and quantitative real-time PCR

We used TRIzol reagent (Invitrogen, Carlsbad, CA, USA) to extract total RNA from cervical cell lines. Then, total RNA was reverse transcribed into cDNA using the HyperScript III RT SuperMix (NovaBio, Shanghai, China). Quantitative PCR (qPCR) was conducted to assess the expression level of MPC1. The primers of MPC1 were 5′- ACTATGTCCGAAGCAAGGATTTC −3′ and 5′- CGCCCACTGATAATCTCTGGAG-3′. The primers were synthesized using TsingKe (Beijing Tsingke Biotech Co., Ltd). GAPDH was used as an internal control.

Interaction network and functional enrichment analysis

The gene ontology (GO) term enrichment analysis was performed using the LinkedOmics database (http://www.linkedomics.org/) pathway analysis. Gene set enrichment analysis (GSEA) v3.0 (http://www.broadinstitute.org/gsea/) was used to investigate significantly enriched immune and metabolism pathways of MPC1 [22, 23]. Furthermore, c2.cp.kegg.v7.2.symbols.gmt (curated) from MsigDB (https://www.gsea-msigdb.org/gsea/msigdb) were used as the reference gene sets [24]. Gene set permutation was performed 1,000 times for each analysis. P values<0.05 and FDR (false discovery rate) q<0.05 were considered threshold values to estimate statistical significance. All diagrams were drawn using R software (version 4.2.1). The network neighborhoods of MPC1 were visualized using ConsensusPathDB-human (http://consensuspathdb.org) [25]. These data currently originate from 32 public resources for interactions. The GeneMANIA online platform (http://genemania.org/) was employed to corroborate the gene interaction network findings and conduct functional enrichment assessment [26]. The utilization of such a platform ensures the validity of the results obtained and facilitates the identification of biological processes and functional pathways related to the investigated gene network.

Ferroptosis analysis

GCH1, GPX4, FSP1and SLC7A11 are important in the ferroptosis pathway [27, 28]. We identified differentially expressed ferroptosis gene regulators between normal cervical tissues and cervical squamous cell carcinoma and Endocervical Adenocarcinoma in FerrDb. We also conducted the correlation analysis between MPC1 and Ferroptosis gene in TIMER2, ncFO (http://www.jianglab.

cn/ncFO/) Database [29], GEPIA Database, and Kaplan–Meier Plotter. And preliminary verification was conducted through qRT-PCR and immunohistochemical analysis.

Statistical analysis

The Kaplan–Meier plotter, OncoLnc, and GEPIA2 databases were used to generate survival plots, with data including either HR and p-values or p-values derived from a log-rank test. Paired and unpaired continuous variables were compared using Student's t-test. One-way ANOVA was used for comparison among multiple groups. The correlation of gene expression was assessed using Spearman's correlation analysis. All data are presented as the means ± SD. P-values < 0.05 were considered statistically significant in all tests.

Results

Identification of ferroptosis-related and immune-related DEGs in Cervical Cancer

Using Weighted Correlation Network Analysis (WGCNA) of TIP cervical cancer data, 2248 genes associated with immunity were selected through the application of a heat map format. (Supplementary Fig. S1). To identify DEGs related to the ferroptosis-related and immune-related gene of cervical cancer, we intersected three GEO datasets (GSE7803, GSE9750, and GSE39001), the FerrDb database, and 2248 immune-related genes. As a result, a total of eight DEGs were identified using an adjusted p-value < 0.05. Venn analysis was performed (Fig. 1). These genes are IDO1, GJA1, SLC16A1, FADS1, NCF2, ALOX12B, MPC1, and AURKA, respectively. After analyzing the correlation between expression and prognosis, MPC1 was ultimately identified as a significant factor (Supplementary Fig. S2).

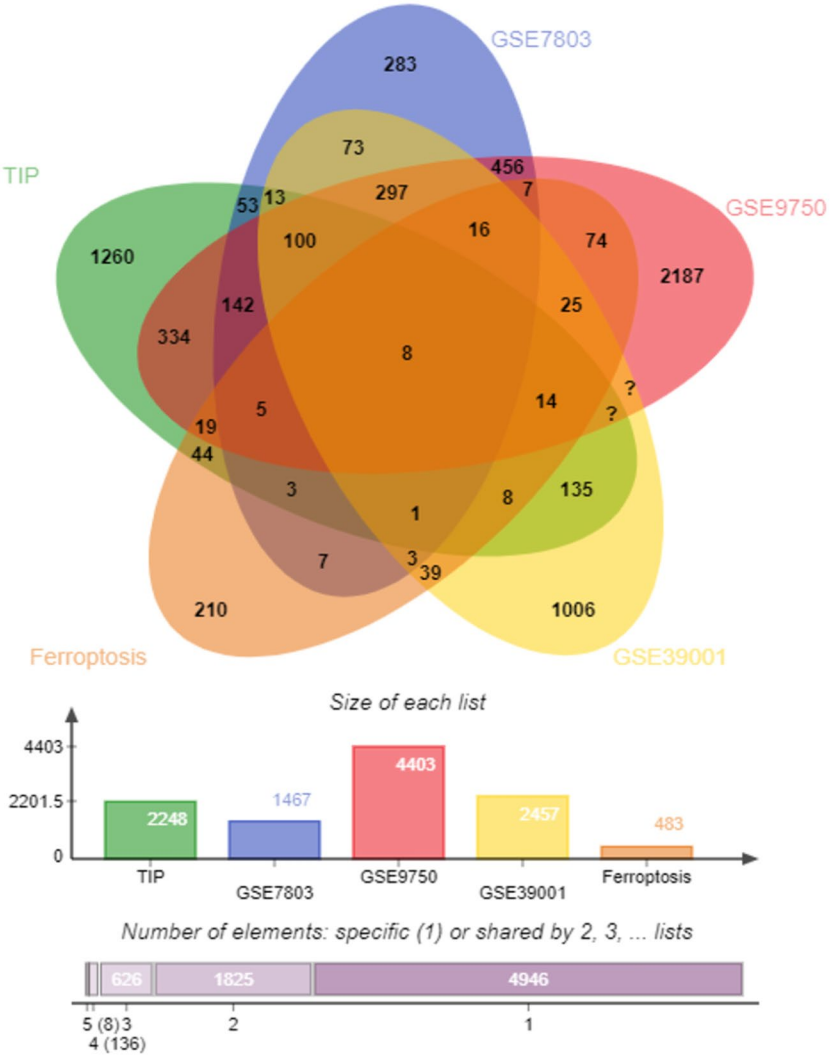

Fig. 1 Identification of ferroptosis-related and immune-related genes in cervical cancer. Co-DEGs identified using Venn diagrams

Expression levels of MPC1 mRNA in cervical squamous cell carcinoma (CESC)

Based on data from the GEPIA database, three GEO datasets (GSE7803, GSE9750, and GSE39001), and the UALCAN database, we assessed the expression of MPC1 in patients with cervical cancer. As shown in Fig. 2A–D and Supplementary Fig. S3A, the MPC1 expression level in CESC was lower than that in normal cervical tissues. We further used the UALCAN database to examine that MPC1 had lower expression levels in metastatic cervical cancer samples than in primary CESC samples using the TNM plotter (Fig. 2E). Furthermore, the expression of MPC1 exhibits a negative correlation with ascending tumor stages (Fig. 2F). Moreover, a meticulous examination of MPC1's expression in CESC was conducted, taking into account variations in tissue histology, as documented in the UALCAN database (Supplementary Fig. S3B). Additionally, the expression of MPC1 was decreased in almost all types of cancer, such as bladder urothelial carcinoma (BLCA), cholangiocarcinoma (CHOL), colon adenocarcinoma (COAD), esophageal carcinoma (ESCA), head and neck squamous cell carcinoma (HNSC), kidney chromophobe (KICH), liver hepatocellular carcinoma (LIHC), lung adenocarcinoma (LUAD), rectum adenocarcinoma (READ), and thyroid carcinoma (THCA) (Supplementary Fig. S3C–D).

Immunohistochemical Analysis

We detected the protein level of MPC1 via IHC in a group of 64 samples, which included 32 normal cervical epithelial and 32 cervical cancer tissues. Next, we analyzed the expression of MPC1 in 32 sets of cervical cancer and adjacent normal epithelial tissues. Normal cervical epithelial samples exhibited stronger staining of MPC1 than did cervical cancer tissues (Fig. 3A). The score for MPC1 was significantly lower in cervical cancer tissues than in adjacent normal tissues (Fig. 3B), and the protein level of MPC1 was decreased in patients who had positive lymph node metastasis (Fig. 3C). Furthermore, in cervical cancer cell lines, the mRNA expression of MPC1 was lower compared to that in normal cervical epithelial cell line H8 (Fig. 3D).

Prognostic value of MPC1 in CESC

The present investigation utilized the TISIDB database and the OncoLnc database to assess the correlation

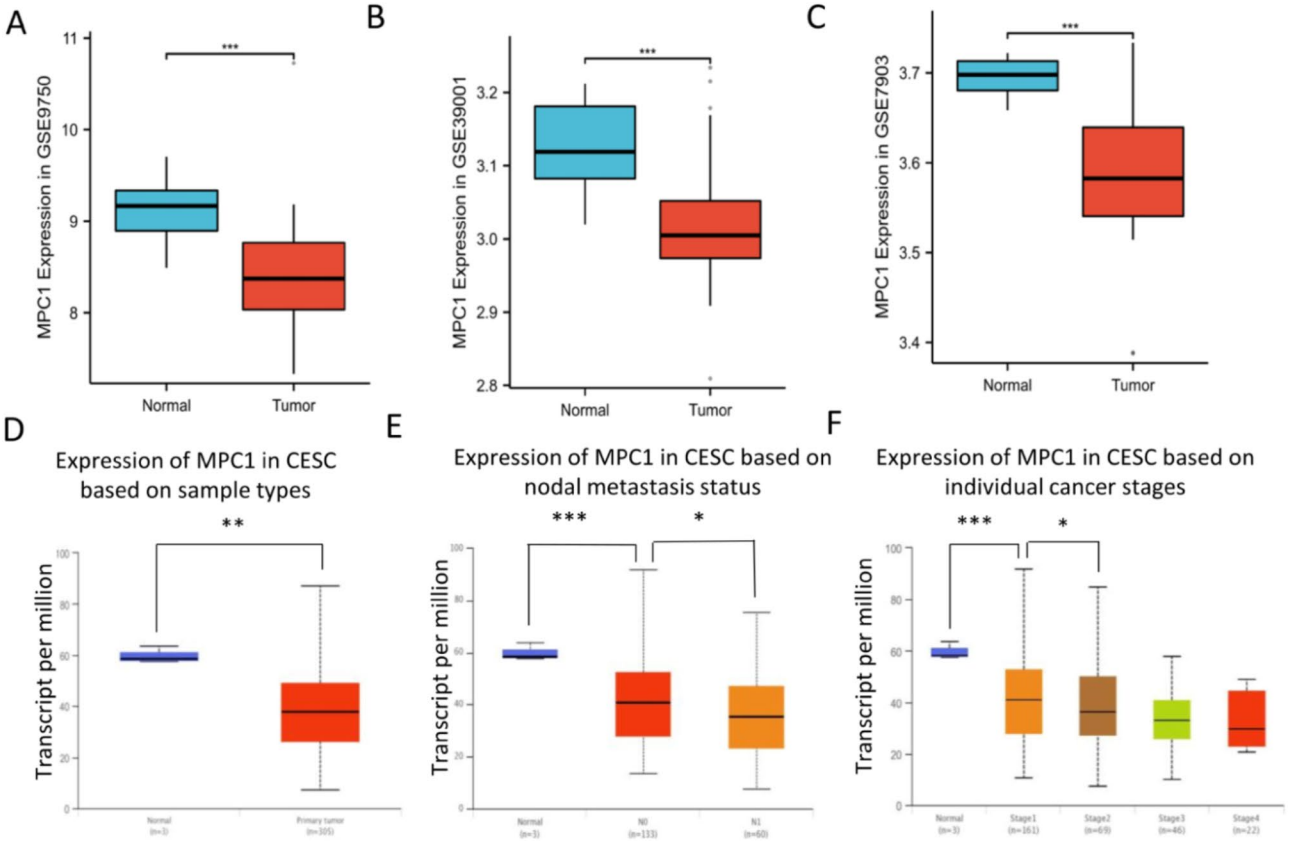

Fig. 2 MPC1 expression levels in cervical cancer. (**A–C**) The expression of MPC1 between CESC and normal tissues of the cervix uteri in three GEO datasets. (**D**) Primary cervical cancer compared with metastatic cervical cancer samples in the UACLAN database. (**E**) MPC1 expression levels in different lymph node metastasis status of CESC from the UACLAN database. (**F**) MPC1 expression levels in different stages of cervical and endocervical cancers from the UALCAN database. *$p < 0.05$, ** $p < 0.01$, ***$p < 0.001$

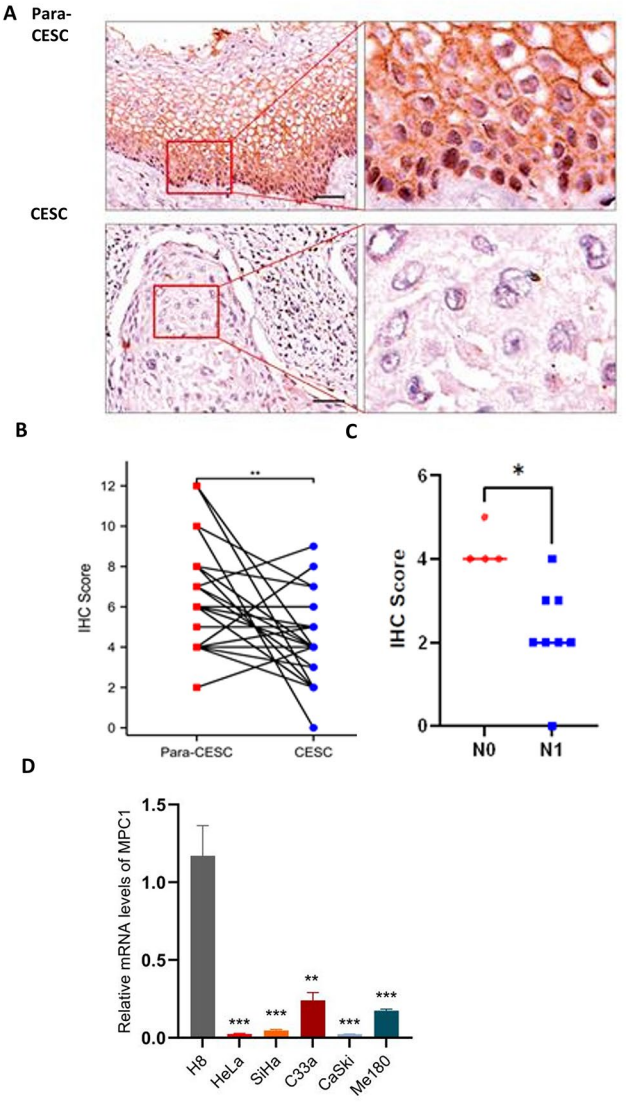

Fig. 3 Protein level and mRNA expression of MPC1 in cervical cancer. (**A**) Protein levels of MPC1 in cervical cancer tissues and adjacent normal epithelial tissues detected using IHC. (**B**) IHC scores between cervical cancer tissues and adjacent normal epithelial tissues. (**C**) IHC scores of MPC1 between N0 ($n=8$) and N1 ($n=4$) of cervical cancer samples. (**D**) qRT-PCR detected MPC1 mRNA expression in normal cervical epithelial cell line H8 and five cervical cancer cell lines

between elevated MPC1 expression and a favorable prognosis in patients diagnosed with cervical cancer (Fig. 4A–B). In this study, we utilized the Kaplan–Meier plotter database to explore the association between MPC1 gene expression and the prognosis of patients with cervical squamous cell carcinoma. The sample size consisted of 304 participants with overall survival (OS) data and 174 participants with progression-free survival (PFS) data. Results indicated a significant positive correlation between MPC1 gene expression and improved OS in this cohort [HR=0.42 (0.26–0.69), $P=0.00042$] (Fig. 4C). However, the gene expression had no statistical significance with PFS [HR=1.9 (0.72–5.14), $P=0.19$] (Fig. 4D). In the Kaplan–Meier plotter databases, RNA sequencing data were also acquired and used for online analysis of the prognostic value of MPC1 in 143 patients with CESC who had diverse tumor mutation statuses. We found that MPC1 levels were positively correlated with OS in patients with high mutation burden (Fig. 4E) and not with low mutation burden (Fig. 4F).

Correlation of MPC1 expression with the tumor-immune microenvironment (TME)

Several investigations have demonstrated that tumor-infiltrating immune cells (TILs) possess prognostic value in relation to cervical cancer [30, 31]. In the TIMER2 database, the present examination revealed a correlation between MPC1 expression and both B-cells and macrophages in the context of CESC (Fig. 5A–B). However, Myeloid dendritic cells, CD8+T cells, and CD4+T cells were not correlated with MPC1 expression (Fig. 5C–E). Specifically, in CESC, under low MPC1 expression, lower B cell levels had a worse outcome using the XCELL algorithm in CESC (HR=0.401, $p=0.0063$) (Fig. 5F). Furthermore, the lower M2 macrophage infiltration level predicted a terrible prognosis under the lower expression of MPC1 in CESC using the QUANTISEQ algorithm (HR=0.4, $p=0.0105$) (Fig. 5G). Additionally, it was determined through comprehensive examinations that the expression of MPC1 in CESC was intricately associated with increased levels of T cells, CD4+T cells, and monocytes (Fig. 5H).

In cervical cancer, cancer-associated fibroblasts (CAFs) are a pivotal constituent of the tumor microenvironment and are distinguished by a remarkable level of adaptability; moreover, CAFs play significant roles in the genesis and advancement of malignancy [32]. The regulation of CAFs functions could be synchronized with immunotherapy [33]. The GEPIA2021 platform revealed consistent results that MPC1 is highly expressed in endothelial cells / CAFs in CESC normal tissue from TCGA using the EPIC algorithm (Fig. 6A). Furthermore, we observed consistent results indicating that MPC1 was highly expressed in CD4_T cells and B cells in CESC tumor/CESC normal from TCGA (Fig. 6B). In addition, we calculated the MPC1 expression of each cell cluster in GSE168652 using TISCH2 (Fig. 6C). Using unsupervised dimensionality reduction and clustering, we identified seven cell subclusters among the 22,998 cells in GSE168652 (Fig. 6D). The seven cell subclusters showed different MPC1 expression levels (Fig. 6E).

Correlation analysis between MPC1 and related markers of immune cells were appraised in cervical cancer (Fig. 7A–B). To further clarify the relationship between MPC1 and various subtypes of TILs in cervical cancer, the TIMER2 online databases were employed to further

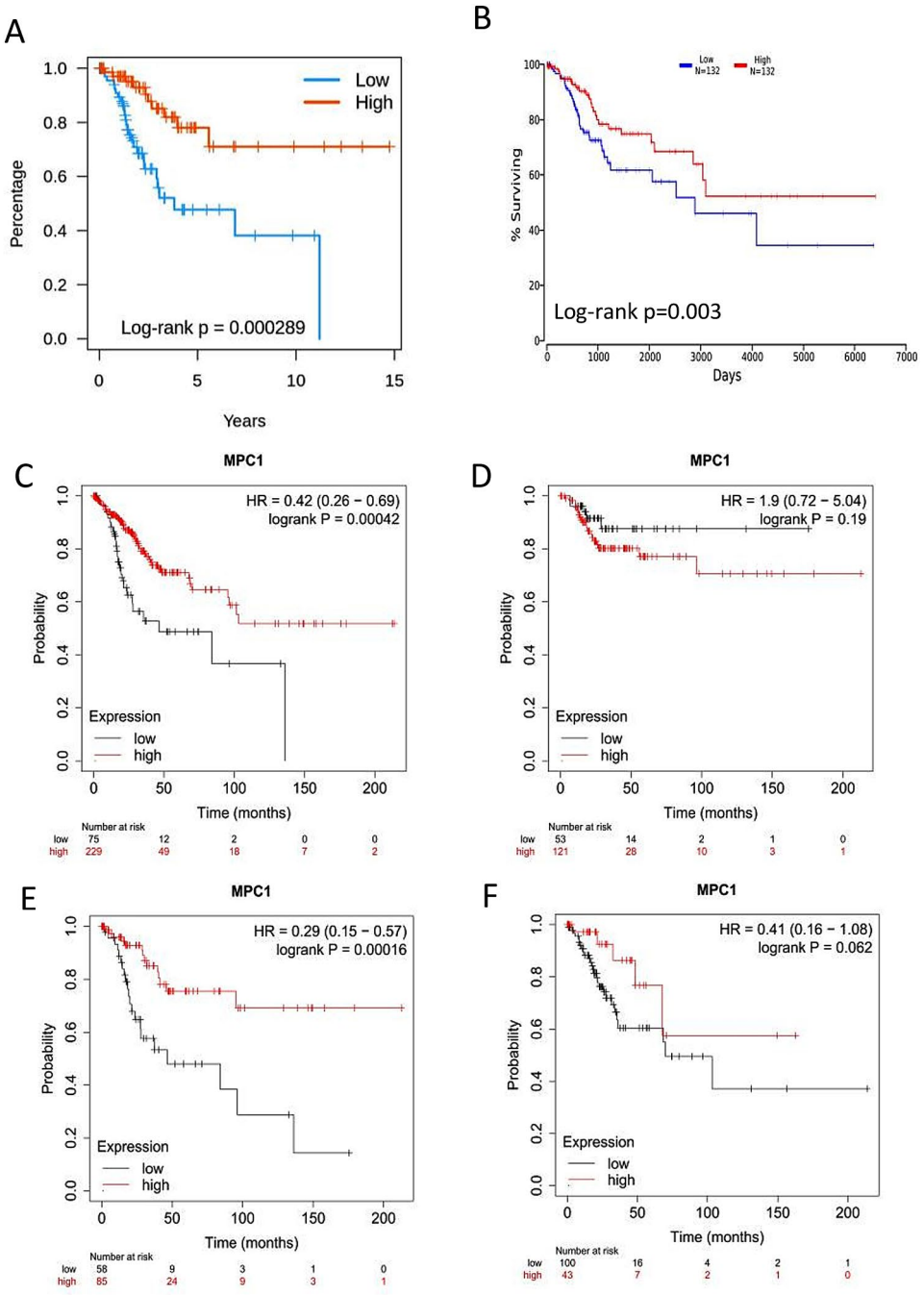

Fig. 4 Kaplan–Meier survival curves comparing high and low expression of MPC1 in CESC (**A–B**) Survival curves of OS in CESC from the TISIDB and OncoLnc database. (**C–D**) Survival curves of OS and PFS in CESC from Kaplan–Meier plotter databases. (**E**) MPC1 expression was correlated with OS in high or (**F**) low tumor mutation burden from the Kaplan–Meier plotter

analyze the relationship between MPC1 and marker genes of different immune cells, including CD8+T cells, CD4+T cells, B cells, macrophages, neutrophils and dendritic cells in cervical cancer (Supplementary Table S1). LGALS9 and VTCN1 were significantly associated with MPC1 expression (Fig. 7C–D). The Kaplan–Meier plotter database was employed to delve into the correlation between the expression of the aforementioned genes and patients' survival outcomes. Our results revealed that high expression of the two genes was significantly associated with increased overall survival, suggesting their potential role as prognostic indicators in CESC (Fig. 7E-F). To explore the expression of LGALS9 and VTCN1 in HeLa cells with MPC1 knockdown, siRNA-targeted MPC1 were designed and transfected into HeLa cells. The efficiency of knockdown was validated using qRT-PCR

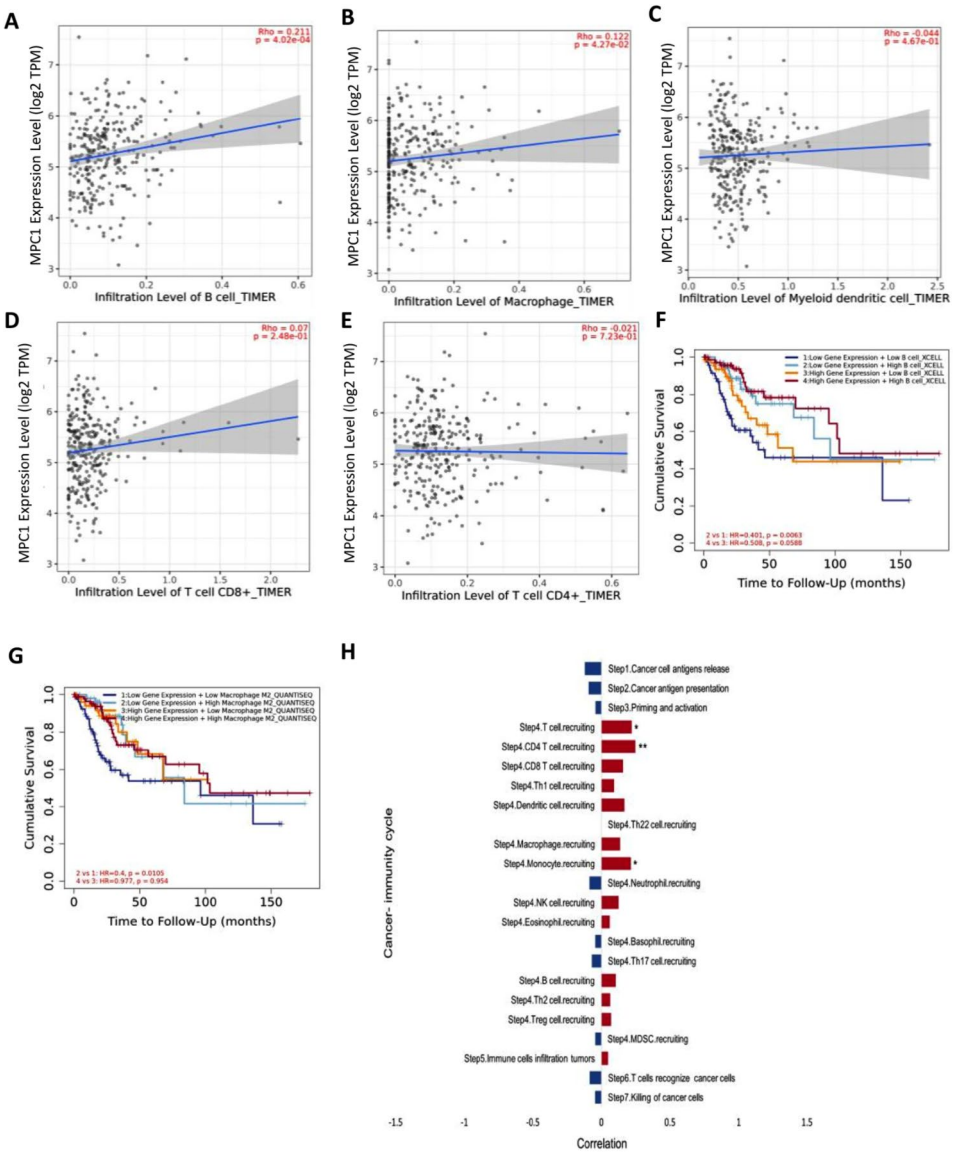

Fig. 5 Correlation of MPC1 expression with immune infiltration level in cervical squamous cell carcinoma cancer (**A–E**). Expression of MPC1 and immune infiltration in TIMER2.0 database. (**F**) Kaplan–Meier curve for the MPC1 expression level and B cell infiltration using the XCELL algorithm in CESC. (**G**) Kaplan–Meier curve for the MPC1 expression level and M2 macrophage infiltration using CIBERSORT algorithm in CESC. (**H**) Comprehensive analysis of immune cells and MPC1 expression

and the efficiency of siMPC1 reaches 40%. The results showed that MPC1 knockdown reduced the expression of LGALS9 and VTCN1 in HeLa cells (Fig. 7G–H).

GSEA identifies MPC1-related signaling pathways

In cervical cancer, the expression of MPC1 has been observed to be intricately linked to diverse metabolic pathways using KEGG pathway-based analysis (Fig. 8A–C). Additionally, Fig. 8D, E present the significant enrichment of signaling pathways associated with low MPC1 expression, as identified through GO analysis and Hallmark analysis.

Ferroptosis analysis

The differential expression of ZEB1 and KIF20A was revealed in FerrDb between normal cervical tissues and those afflicted with cervical squamous cell carcinoma (Fig. 9A). Drivers and inducers positively regulate ferroptosis, while suppressors and inhibitors negatively regulate ferroptosis. The aforementioned genes have significant implications in the pathogenesis of this cancer subtype. The expression of MPC1 exhibits a positive correlation with the presence of ferroptosis genes in TIMER2 (Fig. 9B–E); however, no apparent relationship was observed with SLC7A11 (Fig. 9F). Except for the ZEB1 gene, other expressions of ferroptosis regulators

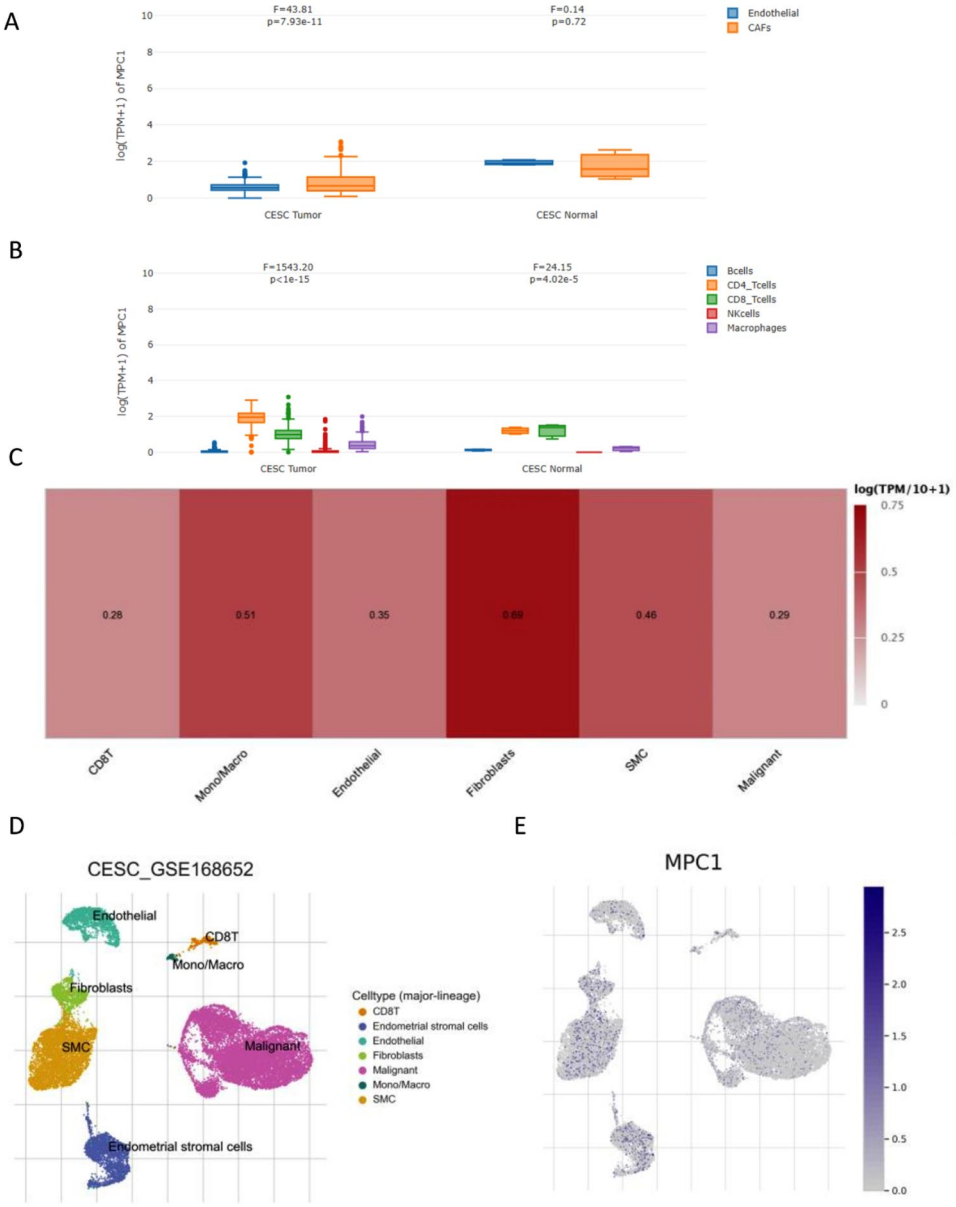

Fig. 6 MPC1 expression in TME-related cells. (**A**) Comparison of the distribution of MPC1 expression in endothelial cells and CAFs in CESC tumor/CESC normal from TCGA. (**B**) Comparison of the distribution of MPC1 expression across samples in CESC tumor/CESC normal from TCGA. (**C–D**) The TME cell types and distribution in the GSE168652_inDrop dataset. (**E**) Distribution of MPC1 in different cell types analyzed with single-cell resolution in the GSE168652_inDrop dataset using the TISCH database

in cervical tumors were higher than those in normal cervical tissue in the TNM plot (Fig. 9G), ncFO (Supplementary Fig. S4A–C), and GEPIA (Supplementary Fig. S4D–E). The prognosis of patients significantly improved as the gene expression increased, as evidenced by data from the Kaplan–Meier plotter databases (Supplementary Fig. S4F–G). Nevertheless, SLC7A11 gene expression contradicts this pattern (Supplementary Fig. S4H) and the prognostic significance of ZEB1 and KIF20A expression remains unclear (Supplementary Fig. S4I-J). To explore the expression of important ferroptosis genes in HeLa cells with MPC1 knockdown, siRNA-targeted MPC1 were designed and transfected into HeLa cells. The efficiency of knockdown was validated using qRT-PCR and the efficiency of siMPC1 reaches 90%. (Fig. 9H). The results showed that MPC1 knockdown markedly reduced the expression of FSP1, GCH1, and GPX4 in HeLa cells. However, the expression of SLC7A11 was almost unaffected (Fig. 9I). We analyzed the expression of FSP1, GCH1 and GPX4 in 32 sets of cervical cancer and adjacent normal epithelial tissues. The staining intensity of the three Ferroptosis genes mentioned above

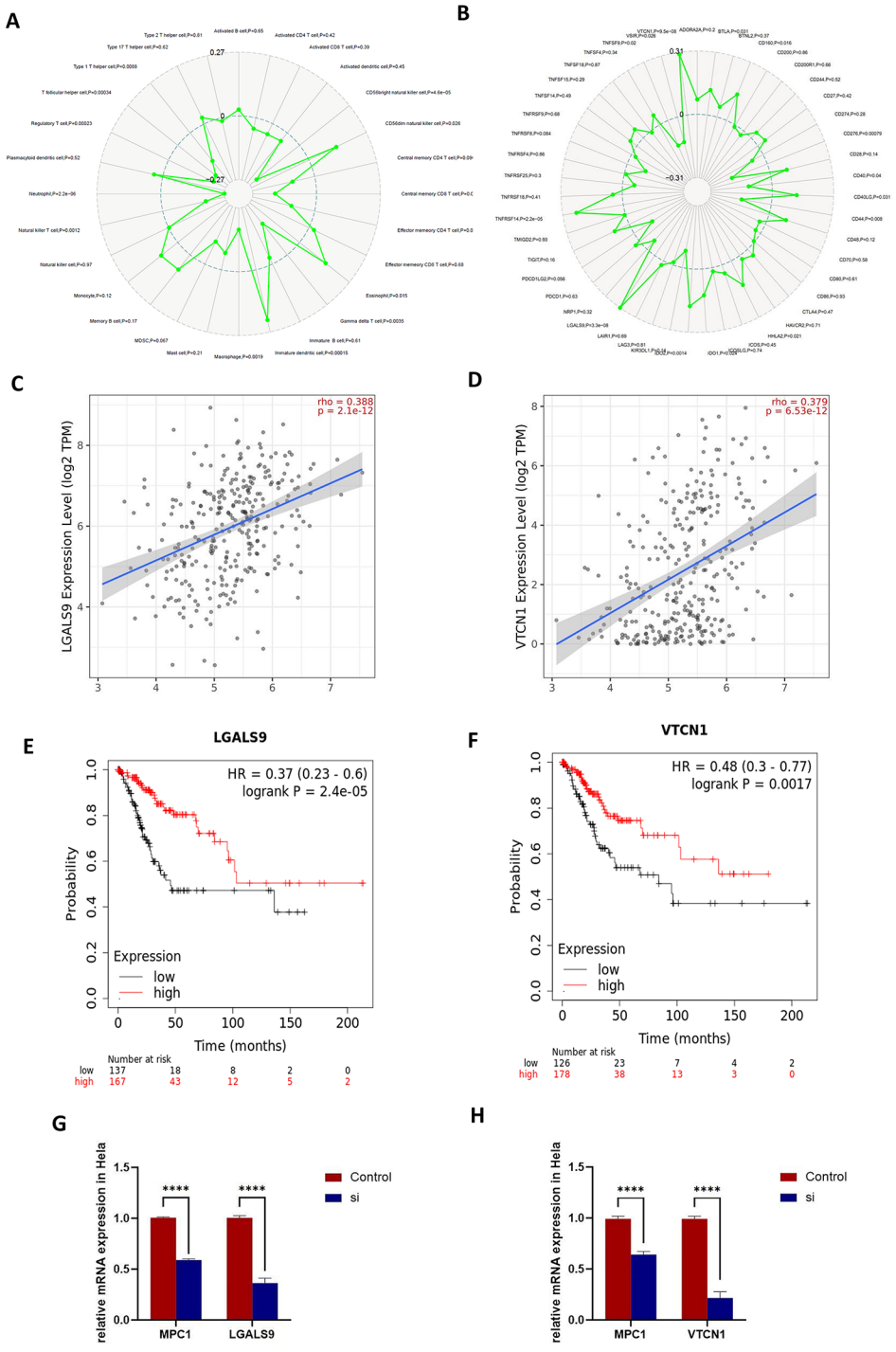

Fig. 7 MPC1 expression and immune checkpoint markers. (**A–B**) Analysis of MPC1 expression with immune checkpoint markers in CESC tumor (**C–D**) MPC1 expression related to the levels of LGALS9 and VTCN1. (**E–F**) Survival curves of OS for CESC obtained from the Kaplan–Meier plotter databases. (**G–H**) qRT-PCR analyzed the expression of LGALS9 and VTCN1 genes with MPC1 downregulation

in cervical cancer tissue are higher than that in normal cervical tissue (Fig. 9J). And the scores for these genes are significantly higher in cervical cancer tissues than in adjacent normal tissues (Fig. 9K).

Gene interaction network of MPC1

To understand the biological function of MPC1 ConsensusPathDB was used to integrate the interaction network of MPC1 in *Homo sapiens*. The network defined the neighborhood-based entity set centered by MPC1

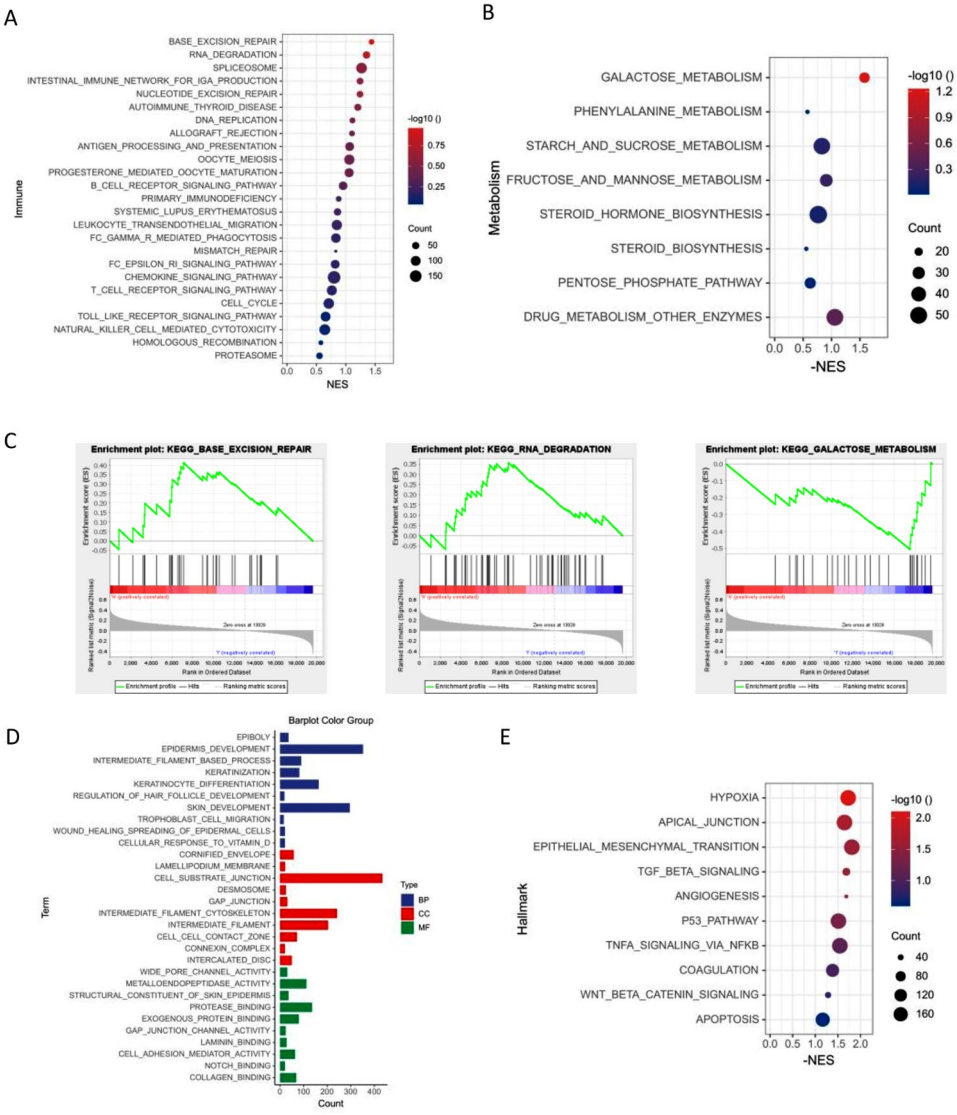

Fig. 8 Function and pathway enrichment analyses using high MPC1 expression (**A**) and low MPC1 expression (**B**) of cervical cancer in TCGA-CESC data. (**C**) Gene set enrichment plots of the signaling pathway in TCGA-CESC data with high or low MPC1 expression. Pathway analysis, utilizing GO (**D**) or Hallmark enrichment (**E**), reveals the first few pathways associated with low MPC1 expression

(Fig. 10A). A gene interaction network was constructed using the GeneMANIA. Twenty MPC1-associated genes were also observed in the interaction network (Fig. 10B). Our analysis revealed that its primary functions are predominantly focused on processes such as pyruvate metabolism and glycolysis, with some degree of association with immunity.

Discussion

MPC1 is a crucial metabolic protein that regulates the transport of pyruvate into the mitochondrial inner membrane. MPC1 deficiency potentially elicits metabolic reprogramming [15]. Studies have shown that MPC1 expression is notably decreased in cancer tissue and is associated with a poor prognosis [34, 35]. MPC1 inhibition increases mesenchymal marker expression, glutaminolysis, and vulnerability to ferroptosis inducers in vitro and in vivo [35].

According to our examination, MPC1 was implicated in the induction of TNM. Moreover, MPC1 serves as a crucial modulator of the neoplastic milieu, and the disruption of its equilibrium is implicated in the initiation and advancement of carcinogenesis. Our initial discovery highlights the promotive roles of B cells, macrophages, VTCN1, and LGALS9 in enhancing the immunological advancements in cervical cancer. B lymphocytes possess dual effects on the prognosis of cervical carcinoma, with convincing evidence indicating that B regulatory proteins exert anti-neoplastic activities in human subjects [36]. M1 macrophages demonstrate anti-neoplastic

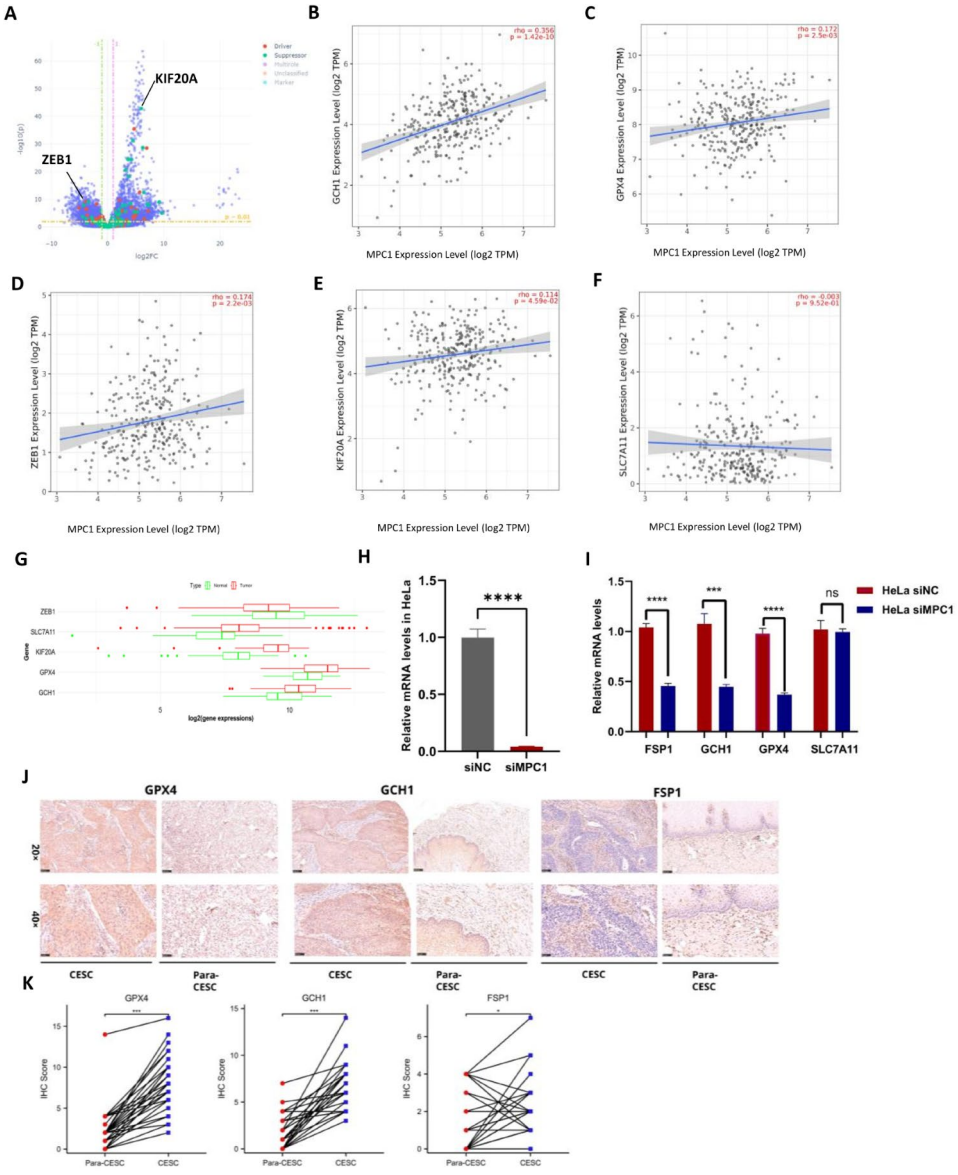

Fig. 9 (**A**) Differentially expressed ferroptosis gene regulator in CESC. (**B–F**) Correlation of ferroptosis genes expression with MPC1 levels in CESC. (**G**) Comparison of ferroptosis gene expression levels between normal cervical tissues and cervical tumors. (**H**) Detection of the efficiency of MPC1 knockdown in HeLa cells using qRT-PCR. (**I**) qRT-PCR analyzed the expression of ferroptosis genes with MPC1 downregulation. (**J**) Protein levels of ferroptosis genes in cervical cancer tissues and adjacent normal epithelial tissues detected using IHC. (**K**) IHC scores between cervical cancer tissues and adjacent normal epithelial tissues

characteristics in certain malignancies, whereas M2 macrophages facilitate tumorigenesis [37]. Neutrophils contribute to tumor progression through intricate mechanisms. Research has demonstrated that an elevated quantity of T lymphocytes in individuals with cervical cancer correlates with a more favorable prognosis [38]. The immune cells in the database have not been further categorized, so the impact of certain immune cell infiltration levels needs further investigation. However, the infiltration levels of B cells and macrophages as well as the expression of MPC1 have implications on the prognosis of cervical cancer patients, prompting our attention. The biological activity of VTCN1(B7-H4 /B7x/B7S1) has been associated with decreased inflammatory CD4+T cell responses and a correlation between VTCN1-expressing tumor-associated macrophages and FoxP3+regulatory T cells (Tregs) within the tumor microenvironment [39]. Some academic publications demonstrate unique intracellular impacts, including reduced apoptosis, increased proliferation, and facilitated metastasis, in cells with VTCN1 expression. In both ovarian carcinoma and breast cancer, studies have indicated that low VTCN1 expression can diminish metastasis and invasion [40, 41]. Nevertheless, our data shows a positive association

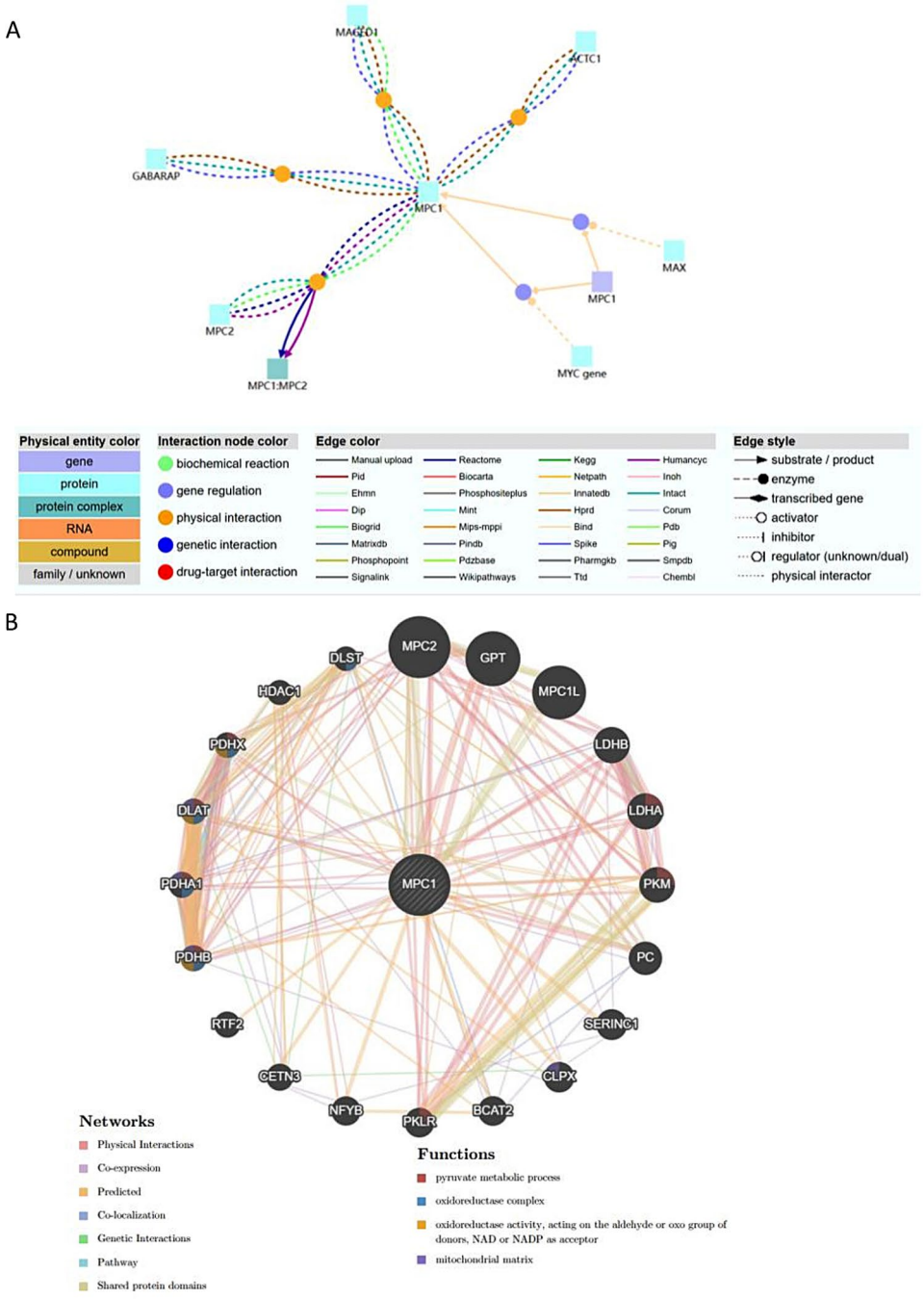

Fig. 10 Gene interaction network of MPC1. (**A**) Gene interaction network of MPC1 using the ConsensusPathDB database. (**B**) Gene interaction network of MPC1 constructed using GeneMANIA

between VTCN1 expression and MPC1 expression, as well as a correlation with improved overall survival in patients with CESC in the bioinformatics analysis conducted in this study. However, further investigations are necessary to confirm these findings. Recent studies have demonstrated that LGALS9 (Galectin-9) regulates immune homeostasis and tumor cell survival through its interaction with its receptor Tim-3 [42–44]. A previous study showed that an oncogenic mutation of KRAS sensitizes CRC cells to autophagy-dependent cell death by a recombinant form of the epithelial polarity regulator LGALS9 in vitro and in vivo [45]. Higher mRNA levels of the LGALS9 gene were detected in HaCaT non-tumor cells, whereas SiHa and HeLa cervical cancer cells, which are derived from cervical squamous cell carcinoma and adenocarcinoma, respectively, exhibited low expression

levels of the gene [46]. In conclusion, the close relationship between MPC1 and LGALS9 might uncover a novel mechanism for inhibiting tumors. Further research into these proteins and their interactions could lead to the development of new therapies for patients with cancer.

There are several established lipid peroxidation-defending systems within cells, including SLC7A11/GPX4 and GCH1/BH4, all of which serve as pathways that prevent ferroptosis [27, 28]. GPX4 is a central regulator of ferroptosis and regulates ferroptosis induced by 12 divergent compounds [47]. The regulation of the KDM5A-MPC1 axis is found to play a significant role in enhancing the susceptibility of cancer cells to ferroptosis. In erPCC, there was an observed increase in KDM5A expression and a decrease in MPC1 expression. Inhibiting KDM5A led to an increase in MPC1 expression and a reduction in sensitivity to ferroptosis inducers. Suppression of MPC1 resulted in an increased vulnerability to ferroptosis both in vitro and in vivo, by maintaining mesenchymal traits and glutaminolysis. Additionally, in shMPC1-transfected tumors, an increase in KDM5A expression and a decrease in GPX4 expression was observed. Furthermore, the suppression of GPX4 and xCT led to an increased sensitivity to ferroptosis in in vivo models of GPX4 genetic silencing [35]. Inhibiting GCH1/BH4 metabolism promoted erastin-induced ferroptosis by activating ferritinophagy, suggesting that combining GCH1 inhibitors with erastin in the treatment of CRC is a novel therapeutic strategy [48]. Moreover, the METTL3-PBX1-GCH1 axis increased BH4 levels in gastric cancer cells, thereby promoting tumor progression [49]. Recent studies have also revealed that SLC7A11 overexpression promotes tumor growth partly through suppressing ferroptosis [50]. Mechanistically, pharmacological inhibition or genetic deletion of PARP downregulates the expression of the cystine transporter, SLC7A11, in a p53-dependent manner in ovarian cancer. Consequently, the repression of SLC7A11 leads to a reduction in glutathione biosynthesis, thereby promoting lipid peroxidation and triggering ferroptosis [51]. In this study, the suppression of MPC1 results in reduced levels of GPX4, GCH1, and FSP1 expression. The low levels of expression of the aforementioned genes have been shown to be associated with potent inhibition of tumor progression. It is plausible that a mechanism exists whereby the co-expression of MPC1 and these three genes confers patients with survival advantages. However, how MPC1 interacts with these pathways is still unclear, which deserves further study. ZEB1 is a key molecule of epithelial-mesenchymal transition (EMT) that plays a significant role in tumor invasion and metastasis. ZEB1 downregulates E-cadherin, which is known as an epithelial marker, through a close relationship with SIRT1 [52]. ZEB1 overexpression has also been shown to increase the susceptibility of cancer cells to ferroptosis [53].

The findings of this study reveal a noteworthy affirmative correlation between the manifestation of MPC1 and the manifestation of ZEB1 in cervical carcinoma. Increased KIF20A accelerated tumor proliferation, invasion, migration, and inhibited apoptosis of tumor cells [54, 55]. Cellular ferroptosis may be inhibited via the KIF20A/NUAK1/PP1β/GPX4 pathway in CRC cells, which may underlie the resistance of CRC to oxaliplatin [56]. In this study, a dialectical incongruity in the genetic expression of MPC1 and KIF20A is evident. The reduced expression of ferroptosis resistance genes in cancer cells renders them more vulnerable to the impact of ferroptosis inducers. This implies that the simultaneous expression of MPC1 and ferroptosis inhibitory genes could result in metabolic reprogramming, heighten the sensitivity of cervical cancer cells to ferroptosis, and potentially confer survival advantages to patients. The relationship between MPC1 and ferroptosis genes needs further exploration by conducting experiments. The genetic interaction network reveals the molecular pathways linked to reduced MPC1 gene expression and unfavorable prognosis in cervical cancer patients, predominantly involving cellular metabolism. These genes will be the focal point of our forthcoming research endeavors. In general, there exists a definite correlation between MPC1 and the tumor microenvironment as well as ferroptosis. However, the limitation of this study is that the exact mechanism of action remains ambiguous, necessitating further analysis and experimental validation.

Conclusions

In our recent research, we discovered that the MPC1 gene is downregulated in cervical cancer—a highly prevalent and devastating form of cancer that affects women worldwide. Our findings reveal that low expression of MPC1 may serve as a potential biomarker for disease progression. In addition to its prognostic potential, MPC1 appears to play a crucial role in regulating the tumor microenvironment (TME). Our study shows that MPC1 may modulate the immune response to cervical cancer by influencing the activities of immune cells and checkpoints. This suggests that targeting MPC1 could be crucial to enhancing the response of the immune system against cervical cancer cells. Importantly, our research also points to a potential relationship between MPC1 and ferroptosis, a novel form of cell death triggered by the accumulation of iron and lipid peroxidation. This suggests that MPC1 may provide a novel therapeutic target for the induction of ferroptosis in cervical cancer.

Abbreviations

MPC1	Mitochondrial Pyruvate Carrier 1
MPC	Mitochondrial Pyruvate Carrier

BAP1	BRCA1-associated Protein 1
CC	cervical Cancer
GO	Gene Ontology
KEGG	Kyoto Encyclopedia of Genes Genomes
GSEA	Gene Set Enrichment Analysis
DEGs	The Differentially Expressed Genes
RM ANOVA	Repeated measures analysis of variance
BRCA	Breast-invasive Carcinoma
CESC	Cervical squamous cell carcinoma and Endocervical Adenocarcinoma
BLCA	Bladder Urothelial Carcinoma
CRC	Colorectal Carcinoma
HCC	Hepatocellular Carcinoma
GBM	Glioblastoma
CHOL	Cholangiocarcinoma
COAD	Colon Adenocarcinoma
ESCA	Esophageal carcinoma,
HNSC	Head and Neck Squamous Cell Carcinoma
KICH	Kidney chromophobe
LIHC	Liver hepatocellular carcinoma
LUAD	Lung adenocarcinoma
READ	Rectum Adenocarcinoma
THCA	Thyroid carcinoma
GEO	Gene Expression Omnibus
WGCNA	Weighted Correlation Network Analysis
TMA	Tissue Microarray
GCH1	GTP Cyclohydrolase-1
GPX4	Glutathione Peroxidase 4
SLC7A11	Solute Carrier Family 7 Member 11
OS	Overall Survival
PFS	Progression-free Survival
TME	The Tumor-immune Microenvironment
TILs	Tumor-infiltrating Immune Cells
CAFs	Cancer-associated Fibroblasts
VTCN1	T-cell Activation Inhibitor-1
LGALS9	Lectin Galactoside-binding Soluble 2
ZEB1	Zinc Finger E-box-binding Homeobox
KIF20A	Kinesin Family Member 20A

Supplementary Information

The online version contains supplementary material available at https://doi.org/10.1186/s12885-024-12622-x.

Supplementary Material 1: Weighted Correlation Network Analysis (WGCNA) of TIP cervical cancer data.

Supplementary Material 2: (A–H) Survival curves of OS in CESC from Kaplan–Meier plotter databases. (I–P) Genes expression level from GEPIA

Supplementary Material 3: (A) MPC1 gene expression level from GEPIA, including 306 TCGA-CESC samples and 13 GTEx normal cervix samples. (B) MPC1 expression in TCGA-CESC based on tumor histology in UALCAN database. Adenosquamous: Cervical adenosquamous carcinoma, Squamous-cel: Cervical squamous cell carcinoma, Endocervical: Endocervical adenocarcinoma of the usual type | Endocervical type of adenocarcinoma, Mucinous: Mucinous adenocarcinoma of endocervical type, Endometrioid: Endometrioid adenocarcinoma of endocervix (C–D) The expression of MPC1 between tumor and adjacent normal tissues across different types of cancers via UACLAN and TIMER platform. *$p < 0.05$, ** $p < 0.01$, ***$p < 0.001$.

Supplementary Material 4: (A–C) The expression of GCH1, GPX4 and SLC7A11 between cervical tumor and normal cervical tissue in ncFO. (D–E) The expression of ZEB1 and KIF20A between cervical tumor and normal cervical tissue in GEPIA. (F–J) Survival curves of ferroptosis genes OS in Cervical squamous cell carcinoma from Kaplan–Meier plotter databases.

Supplementary Material 5

Acknowledgements
We thank the editors and reviewers for their time spent handling and reviewing this manuscript. We wish to express our recognition to the GEO database for granting access to their platforms and to the contributors who generously uploaded their meaningful datasets. We also acknowledge the TGGA, FerrDb, TIP, UALCAN, TIMER2, GEPIA2, Kaplan–Meier Plotter database, ConsensusPathDB and GeneMANIA KEGG database for providing public data and the Venn diagram tool, GSEA software and Cytoscape software for providing analytical tools.

Author contributions
LM: Conceived and designed the study, Analyzed the data, Interpreted/analyzed the data and results, experimental operation Wrote the paperXTH: Analyzed the data and experimental operationYR: Conceived and designed the study, Analyzed the dataMiao Li and Tianhan Xu contributed equally to this work.WXY (Corresponding Author): Conceptualization, Resources, Supervision, Writing - Review and Editing.ZJW (Corresponding Author): Conceptualization, Resources, Supervision, Writing - Review and Editing.WSF (Corresponding Author): Conceptualization, Funding Acquisition, Resources, Supervision, Writing - Review and Editing.Xiaoyun Wang, Jiawen Zhang and Sufang Wu contributed equally to this work.All authors discussed the results and agreed to be accountable for all aspects of the work. All authors contributed to the article and approved the submitted version.

Funding
This study was supported by Grants from the National Natural Science Foundation of China [82272334].

Data availability
The raw data of the three microarray datasets (accession numbers GSE9750, GSE39001 and GSE7903) were downloaded from the GEO repository (https://www.ncbi.nlm.nih.gov/geo/). All data are publicly accessible. The original contributions presented in the study are included in the article/Supplementary Material. Further inquiries can be directed to the corresponding authors.

Declarations

Ethics approval and consent to participate
The study was reviewed and approved by the Ethics Committee of Shanghai General Hospital. The patients/participants provided their written informed consent to participate in this study.

Consent for publication
Not applicable.

Competing interests
The authors declare no competing interests.

Received: 8 January 2024 / Accepted: 9 July 2024
Published online: 10 October 2024

References

1. Bedell SL, Goldstein LS, Goldstein AR, Goldstein AT. Cervical Cancer screening: past, Present, and Future. Sex Med Rev. 2020;8(1):28–37. https://doi.org/10.1016/j.sxmr.2019.09.005.
2. Franciosi MLM, do Carmo TIT, Zanini D, Cardoso AM. Inflammatory profile in cervical cancer: influence of purinergic signaling and possible therapeutic targets. Inflamm Res. 2022;71(5–6):555–64. https://doi.org/10.1007/s00011-022-01560-8.
3. Boon SS, Luk HY, Xiao C, Chen Z, Chan PKS. Review of the Standard and Advanced Screening, Staging Systems and Treatment modalities for Cervical Cancer. Cancers (Basel). 2022;14(12). https://doi.org/10.3390/cancers14122913.
4. Rimel BJ, Kunos CA, Macioce N, Temkin SM. Current gaps and opportunities in screening, prevention, and treatment of cervical cancer. Cancer. 2022;128(23):4063–73. https://doi.org/10.1002/cncr.34487.
5. Arip M, Tan LF, Jayaraj R, Abdullah M, Rajagopal M, Selvaraja M. Exploration of biomarkers for the diagnosis, treatment and prognosis of cervical

cancer: a review. Discov Oncol. 2022;13(1):91. https://doi.org/10.1007/s12672-022-00551-9.
6. Lei G, Zhuang L, Gan B. Targeting ferroptosis as a vulnerability in cancer. Nat Rev Cancer. 2022;22(7):381–96. https://doi.org/10.1038/s41568-022-00459-0.
7. Liang D, Minikes AM, Jiang X. Ferroptosis at the intersection of lipid metabolism and cellular signaling. Mol Cell. 2022;82(12):2215–27. https://doi.org/10.1016/j.molcel.2022.03.022.
8. Liu J, Kang R, Tang D. Signaling pathways and defense mechanisms of ferroptosis. FEBS J. 2022;289(22):7038–50. https://doi.org/10.1111/febs.16059.
9. McCommis KS, Finck BN. The hepatic mitochondrial pyruvate carrier as a Regulator of systemic metabolism and a therapeutic target for treating metabolic disease. Biomolecules. 2023;13(2). https://doi.org/10.3390/biom13020261.
10. Ruiz-Iglesias A, Manes S. The importance of mitochondrial pyruvate carrier in Cancer Cell Metabolism and Tumorigenesis. Cancers (Basel). 2021;13(7). https://doi.org/10.3390/cancers13071488.
11. Tian GA, Xu CJ, Zhou KX, Zhang ZG, Gu JR, Zhang XL, et al. MPC1 Deficiency promotes CRC Liver Metastasis via Facilitating Nuclear translocation of beta-catenin. J Immunol Res. 2020;2020:8340329. https://doi.org/10.1155/2020/8340329.
12. Ma X, Cui Y, Zhou H, Li Q. Function of mitochondrial pyruvate carriers in hepatocellular carcinoma patients. Oncol Lett. 2018;15(6):9110–6. https://doi.org/10.3892/ol.2018.8466.
13. Wang C, Dong L, Li X, Li Y, Zhang B, Wu H, et al. The PGC1alpha/NRF1-MPC1 axis suppresses tumor progression and enhances the sensitivity to sorafenib/doxorubicin treatment in hepatocellular carcinoma. Free Radic Biol Med. 2021;163:141–52. https://doi.org/10.1016/j.freeradbiomed.2020.11.035.
14. Chai Y, Wang C, Liu W, Fan Y, Zhang Y. MPC1 deletion is associated with poor prognosis and temozolomide resistance in glioblastoma. J Neurooncol. 2019;144(2):293–301. https://doi.org/10.1007/s11060-019-03226-8.
15. Xue C, Li G, Bao Z, Zhou Z, Li L. Mitochondrial pyruvate carrier 1: a novel prognostic biomarker that predicts favourable patient survival in cancer. Cancer Cell Int. 2021;21(1):288. https://doi.org/10.1186/s12935-021-01996-8.
16. Barrett T, Wilhite SE, Ledoux P, Evangelista C, Kim IF, Tomashevsky M, et al. NCBI GEO: archive for functional genomics data sets—update. Nucleic Acids Res. 2012;41(D1):D991–5. https://doi.org/10.1093/nar/gks1193.
17. Zhou N, Bao J. FerrDb: a manually curated resource for regulators and markers of ferroptosis and ferroptosis-disease associations. Database (Oxford). 2020;2020. https://doi.org/10.1093/database/baaa021.
18. Xu L, Deng C, Pang B, Zhang X, Liu W, Liao G, et al. TIP: a web server for resolving Tumor Immunophenotype profiling. Cancer Res. 2018;78(23):6575–80. https://doi.org/10.1158/0008-5472.CAN-18-0689.
19. Ru B, Wong CN, Tong Y, Zhong JY, Zhong SSW, Wu WC, et al. TISIDB: an integrated repository portal for tumor-immune system interactions. Bioinformatics. 2019;35(20):4200–2. https://doi.org/10.1093/bioinformatics/btz210.
20. Zhang Z, Xiang K, Tan L, Du X, He H, Li D, et al. Identification of critical genes associated with radiotherapy resistance in cervical cancer by bioinformatics. Front Oncol. 2022;12:967386. https://doi.org/10.3389/fonc.2022.967386.
21. Liao W, Li W, Li Y, Liu T, Wang Y, Feng D, et al. Diagnostic, prognostic, and immunological roles of CD177 in cervical cancer. J Cancer Res Clin Oncol. 2023;149(1):173–89. https://doi.org/10.1007/s00432-022-04465-5.
22. Jiline M, Matwin S, Turcotte M. Annotation concept synthesis and enrichment analysis: a logic-based approach to the interpretation of high-throughput experiments. Bioinformatics. 2011;27(17):2391–8. https://doi.org/10.1093/bioinformatics/btr337.
23. Wu B, Xi S. Bioinformatics analysis of differentially expressed genes and pathways in the development of cervical cancer. BMC Cancer. 2021;21(1):733. https://doi.org/10.1186/s12885-021-08412-4.
24. Liberzon A, Birger C, Thorvaldsdottir H, Ghandi M, Mesirov JP, Tamayo P. The Molecular signatures database (MSigDB) hallmark gene set collection. Cell Syst. 2015;1(6):417–25. https://doi.org/10.1016/j.cels.2015.12.004.
25. Kamburov A, Wierling C, Lehrach H, Herwig R. ConsensusPathDB–a database for integrating human functional interaction networks. Nucleic Acids Res. 2009;37(Database issue):D623–8. https://doi.org/10.1093/nar/gkn698.
26. Franz M, Rodriguez H, Lopes C, Zuberi K, Montojo J, Bader GD, et al. GeneMANIA update 2018. Nucleic Acids Res. 2018;46(W1):W60–4. https://doi.org/10.1093/nar/gky311.
27. Gao M, Fan K, Chen Y, Zhang G, Chen J, Zhang Y. Understanding the mechanistic regulation of ferroptosis in cancer: the gene matters. J Genet Genomics. 2022;49(10):913–26. https://doi.org/10.1016/j.jgg.2022.06.002.
28. Xu L, Liu Y, Chen X, Zhong H, Wang Y. Ferroptosis in life: to be or not to be. Biomed Pharmacother. 2023;159:114241. https://doi.org/10.1016/j.biopha.2023.114241.
29. Zhou S, Huang YE, Xing J, Zhou X, Chen S, Chen J, et al. ncFO: a Comprehensive Resource of Curated and predicted ncRNAs Associated with Ferroptosis. Genomics Proteom Bioinf. 2022. https://doi.org/10.1016/j.gpb.2022.09.004.
30. Wei E, Reisinger A, Li J, French LE, Clanner-Engelshofen B, Reinholz M. Integration of scRNA-Seq and TCGA RNA-Seq to analyze the heterogeneity of HPV + and HPV- cervical Cancer Immune cells and establish molecular risk models. Front Oncol. 2022;12:860900. https://doi.org/10.3389/fonc.2022.860900.
31. Yu S, Li X, Zhang J, Wu S. Development of a Novel Immune infiltration-based gene signature to Predict Prognosis and Immunotherapy response of patients with cervical Cancer. Front Immunol. 2021;12:709493. https://doi.org/10.3389/fimmu.2021.709493.
32. Fang Z, Meng Q, Xu J, Wang W, Zhang B, Liu J, et al. Signaling pathways in cancer-associated fibroblasts: recent advances and future perspectives. Cancer Commun (Lond). 2023;43(1):3–41. https://doi.org/10.1002/cac2.12392.
33. Kennel KB, Bozlar M, De Valk AF, Greten FR. Cancer-Associated fibroblasts in inflammation and Antitumor Immunity. Clin Cancer Res. 2023;29(6):1009–16. https://doi.org/10.1158/1078-0432.CCR-22-1031.
34. Takaoka Y, Konno M, Koseki J, Colvin H, Asai A, Tamari K, et al. Mitochondrial pyruvate carrier 1 expression controls cancer epithelial-mesenchymal transition and radioresistance. Cancer Sci. 2019;110(4):1331–9. https://doi.org/10.1111/cas.13980.
35. You JH, Lee J, Roh JL. Mitochondrial pyruvate carrier 1 regulates ferroptosis in drug-tolerant persister head and neck cancer cells via epithelial-mesenchymal transition. Cancer Lett. 2021;507:40–54. https://doi.org/10.1016/j.canlet.2021.03.013.
36. Sarvaria A, Madrigal JA, Saudemont A. B cell regulation in cancer and anti-tumor immunity. Cell Mol Immunol. 2017;14(8):662–74. https://doi.org/10.1038/cmi.2017.35.
37. Fridman WH, Zitvogel L, Sautes-Fridman C, Kroemer G. The immune contexture in cancer prognosis and treatment. Nat Rev Clin Oncol. 2017;14(12):717–34. https://doi.org/10.1038/nrclinonc.2017.101.
38. Lippens L, Van Bockstal M, De Jaeghere EA, Tummers P, Makar A, De Geyter S, et al. Immunologic impact of chemoradiation in cervical cancer and how immune cell infiltration could lead toward personalized treatment. Int J Cancer. 2020;147(2):554–64. https://doi.org/10.1002/ijc.32893.
39. Podojil JR, Miller SD. Potential targeting of B7-H4 for the treatment of cancer. Immunol Rev. 2017;276(1):40–51. https://doi.org/10.1111/imr.12530.
40. Gao A, Zhang L, Chen X, Chen Y, Xu Z, Liu Y, et al. Effect of VTCN1 on progression and metastasis of ovarian carcinoma in vitro and vivo. Biomed Pharmacother. 2015;73:129–34. https://doi.org/10.1016/j.biopha.2015.05.016.
41. Iizuka A, Nonomura C, Ashizawa T, Kondou R, Ohshima K, Sugino T, et al. A T-cell-engaging B7-H4/CD3-bispecific fab-scfv antibody targets human breast Cancer. Clin Cancer Res. 2019;25(9):2925–34. https://doi.org/10.1158/1078-0432.CCR-17-3123.
42. Lv Y, Ma X, Ma Y, Du Y, Feng J. A new emerging target in cancer immunotherapy: Galectin-9 (LGALS9). Genes Dis. 2023;10(6):2366–82. https://doi.org/10.1016/j.gendis.2022.05.020.
43. Ma L, Heinrich S, Wang L, Keggenhoff FL, Khatib S, Forgues M, et al. Multiregional single-cell dissection of tumor and immune cells reveals stable lock-and-key features in liver cancer. Nat Commun. 2022;13(1):7533. https://doi.org/10.1038/s41467-022-35291-5.
44. Ou Z, Lin S, Qiu J, Ding W, Ren P, Chen D, et al. Single-nucleus RNA sequencing and spatial transcriptomics reveal the immunological microenvironment of cervical squamous cell carcinoma. Adv Sci (Weinh). 2022;9(29):e2203040. https://doi.org/10.1002/advs.202203040.
45. Wiersma VR, de Bruyn M, Wei Y, van Ginkel RJ, Hirashima M, Niki T, et al. The epithelial polarity regulator LGALS9/galectin-9 induces fatal frustrated autophagy in KRAS mutant colon carcinoma that depends on elevated basal autophagic flux. Autophagy. 2015;11(8):1373–88. https://doi.org/10.1080/15548627.2015.1063767.
46. Armenta-Castro E, Reyes-Vallejo T, Maximo-Sanchez D, Herrera-Camacho I, Lopez-Lopez G, Reyes-Carmona S, et al. Histone H3K9 and H3K14 acetylation at the promoter of the LGALS9 gene is associated with mRNA levels in cervical cancer cells. FEBS Open Bio. 2020;10(11):2305–15. https://doi.org/10.1002/2211-5463.12973.
47. Yang WS, SriRamaratnam R, Welsch ME, Shimada K, Skouta R, Viswanathan VS, et al. Regulation of ferroptotic cancer cell death by GPX4. Cell. 2014;156(1–2):317–31. https://doi.org/10.1016/j.cell.2013.12.010.
48. Hu Q, Wei W, Wu D, Huang F, Li M, Li W, et al. Blockade of GCH1/BH4 Axis activates Ferritinophagy to mitigate the resistance of Colorectal Cancer to

Erastin-Induced ferroptosis. Front Cell Dev Biol. 2022;10:810327. https://doi.org/10.3389/fcell.2022.810327.
49. Liu Y, Zhai E, Chen J, Qian Y, Zhao R, Ma Y, et al. M(6) A-mediated regulation of PBX1-GCH1 axis promotes gastric cancer proliferation and metastasis by elevating tetrahydrobiopterin levels. Cancer Commun (Lond). 2022;42(4):327–44. https://doi.org/10.1002/cac2.12281.
50. Koppula P, Zhuang L, Gan B. Cystine transporter SLC7A11/xCT in cancer: ferroptosis, nutrient dependency, and cancer therapy. Protein Cell. 2021;12(8):599–620. https://doi.org/10.1007/s13238-020-00789-5.
51. Hong T, Lei G, Chen X, Li H, Zhang X, Wu N, et al. PARP inhibition promotes ferroptosis via repressing SLC7A11 and synergizes with ferroptosis inducers in BRCA-proficient ovarian cancer. Redox Biol. 2021;42:101928. https://doi.org/10.1016/j.redox.2021.101928.
52. Lee J, You JH, Kim MS, Roh JL. Epigenetic reprogramming of epithelial-mesenchymal transition promotes ferroptosis of head and neck cancer. Redox Biol. 2020;37:101697. https://doi.org/10.1016/j.redox.2020.101697.
53. Wang X, Liu M, Chu Y, Liu Y, Cao X, Zhang H, et al. O-GlcNAcylation of ZEB1 facilitated mesenchymal pancreatic cancer cell ferroptosis. Int J Biol Sci. 2022;18(10):4135–50. https://doi.org/10.7150/ijbs.71520.
54. Jin Z, Peng F, Zhang C, Tao S, Xu D, Zhu Z. Expression, regulating mechanism and therapeutic target of KIF20A in multiple cancer. Heliyon. 2023;9(2):e13195. https://doi.org/10.1016/j.heliyon.2023.e13195.
55. He H, Liang L, Huang J, Jiang S, Liu Y, Sun X, et al. KIF20A is associated with clinical prognosis and synergistic effect of gemcitabine combined with ferroptosis inducer in lung adenocarcinoma. Front Pharmacol. 2022;13. https://doi.org/10.3389/fphar.2022.1007429.
56. Yang C, Zhang Y, Lin1 S, Liu3 Y. Li1 W. suppressing the KIF20A/NUAK1/Nrf2/GPX4 signaling pathway induces ferroptosis and enhances the sensitivity of colorectal cancer to oxaliplatin. 2021; https://doi.org/10.18632/aging.202774.

Publisher's Note